



- 1 Real-time monitoring of nitrate transport in deep vadose zone under a crop
- 2 field—implications for groundwater protection
- 3
- 4 T. Turkeltaub<sup>a</sup>\*, D. Kurtzman<sup>b</sup>, O. Dahan<sup>a</sup>
- 5
- 6 <sup>a</sup> Department of Hydrology & Microbiology, Zuckerberg Institute for Water Research,
- 7 Blaustein Institutes for Desert Research, Ben Gurion University of the Negev, Sde
- 8 Boker Campus, Negev 84990, Israel
- 9 <sup>b</sup> Institute of Soil, Water and Environmental Sciences, The Volcani Center,
- 10 Agricultural Research Organization, P.O. Box 6, Bet Dagan 50250, Israel
- 11
- 12 \*Corresponding author (tuviat@post.bgu.ac.il)
- 13 Tel.: 972-8-6485012; Mobile: 972-52-3584844; Fax: 972-8-6563504





# 14 Abstract

15	Nitrate is considered the most common non-point pollutant in groundwater. It is often
16	attributed to agricultural management, when excess application of nitrogen fertilizer
17	leaches below the root zone and is eventually transported as nitrate through the
18	unsaturated zone to the water table. A lag time of years to decades between processes
19	occurring in the root zone and their final imprint on groundwater quality prevents
20	proper decision-making on land use and groundwater-resource management. In this
21	study, water flow and solute transport through the deep vadose zone underlying an
22	agricultural field were monitored using a vadose-zone monitoring system (VMS).
23	Data obtained by the VMS over a period of 6 years allowed detailed tracking of water
24	percolation and nitrate migration from the surface through the entire deep vadose zone
25	to the water table at 18 m depth. The temporal variations in the vadose zone sediment
26	water content were used to evaluate the link between rain patterns and water fluxes. A
27	nitrate concentration time series, which varied with time and depth, revealed-in real
28	time—a major pulse of nitrate mass propagating down through the vadose zone from
29	the root zone toward the water table. Analysis of stable nitrate isotopes indicated that
30	manure is the prevalent source of nitrate in the deep vadose zone, and these isotopes
31	were barely affected by natural soil or industrial nitrogen components. Total nitrate
32	mass estimations and simulated pore-water velocity using the analytical solution of
33	the convection-dispersion equation indicated dominance of nitrate vertical transport,
34	and excluded the possibility of lateral nitrate input. Accordingly, prevention of
35	groundwater pollution from surface sources such as agriculture has to include
36	effective and continuous monitoring of the entire vadose zone.
37	

38





39 Keywords: Nitrate transport, Deep percolation, Vadose zone, Groundwater pollution





## 41 **1 Introduction**

43	Groundwater contamination by nitrate originating from agricultural land use is
44	a global problem. The World Health Organization guideline for maximum level of
45	nitrate in the drinking water is 50 mg/L NO <sub>3</sub> . The US Environmental Protection
46	Agency (EPA) regards nitrate as requiring immediate action whenever its
47	concentration exceeds drinking-water standards (US EPA, 1994). A detailed
48	framework was established by the Nitrate Directive of the EC (European Community,
49	1991) to prevent water pollution by nitrate. Nevertheless, nitrate contamination has
50	disqualified drinking-water wells in Israel (local standard: 70 mg/L NO <sub>3</sub> ) more than
51	any other contaminant at the beginning of the 21st century (Elhanany, 2009). To
52	prevent excessive leaching of nitrate and its arrival to the groundwater, it is essential
53	to investigate and quantify the mechanism controlling nitrate migration in the
54	unsaturated zone with respect to the specific agrotechnical regime implemented on
55	land surface.
56	Nitrate fate in the subsurface has been investigated by various approaches,
57	such as: (i) isotopic signature in groundwater systems (Kaplan and Magaritz, 1986;
58	Wassenaar, 1995; Oren et al, 2004; Wassenaar et al., 2006; Showers et al., 2008;
59	Dejwakh et al., 2012; Baram et al., 2013), (ii) crop-management strategies, which
60	combine crop production and nitrate leaching to the subsurface (Leenhardt et al.,
61	1998a, 1998b; Hanson et al., 2006; Doltra and Muñoz, 2010; Beggs et al., 2011), and
62	(iii) studies based on data from the deep vadose zone (Onsoy et al., 2005; Green et al.,
63	2008; Dann et al., 2010; Nolan et al., 2010; Botros et al., 2012; Kurtzman et al., 2013;
64	Dahan et al., 2014; Turkeltaub et al., 2014, 2015a, 2015b).





65	Nitrogen is an essential nutrient for crop growth and is widely used as a
66	fertilizer. Although the dominant forms of soluble nitrogen fertilizer are reduced (e.g.
67	urea, ammonia) and evolve into other nitrogen species through biochemical processes
68	in the soil, nitrate is the most common chemical contaminant in the deep vadose zone
69	and groundwater (Green et al., 2008; Rupert, 2008). The transfer time of nitrate within
70	the deep vadose zone has been estimated to take from weeks to decades, depending on
71	the water regime, thickness of the unsaturated zone and lithological characteristics of
72	the subsurface (Spalding et al., 2001; Scanlon et al., 2010). Moreover, estimates of
73	cumulative nitrate fluxes in the unsaturated zone have shown significant differences in
74	the timing and magnitude of fluxes derived from different land uses (Green et al.,
75	2008; Dahan et al., 2014; Turkeltaub et al., 2014, 2015a, 2015b). Therefore, the
76	cumulative impact of nitrate leaching from the root zone through the unsaturated zone
77	on nitrate level in the groundwater is blurred by mixing and dilution in the aquifer
78	water. The tendency toward elevated nitrate concentration in aquifer water is thus a
79	relatively slow process (Green et al., 2008).
80	Although sampling groundwater from wells is easy, the concentration of
81	nitrate might already be at levels that will lead to disqualification of the aquifer water.
82	Knowing the time lag between initiation of a pollution process in the unsaturated zone
83	and its final impact on aquifer quality could give decision-makers more time to plan
84	possible backups for alternative water supply (Baram et al., 2014). Accordingly,
85	estimations of water and solute fluxes which are based on data from the deep
86	unsaturated zone could better indicate their potential long-term impact on the
87	groundwater (Scanlon et al., 2002; Onsoy et al., 2005; Green et al., 2008).
88	Nevertheless, most of these estimates are based on data obtained from excavated soil
89	profiles or pore-water sampling over a short period of time, which represent a





90	snapshot in time of the sediment's chemical state rather than dynamic temporal
91	variations. Furthermore, knowledge of nitrate's fate and transport below the root zone
92	is restricted due to issues such as soil spatial variability and long travel times in the
93	deep vadose zone (Onsoy et al., 2005).
94	The recent development of a vadose-zone monitoring system (VMS) enables
95	continuous monitoring of the hydrological and chemical properties of percolating
96	water in the deep vadose zone. Data collected by the system comprise direct
97	measurements of the water-percolation fluxes and the chemical evolution of the
98	percolating water across the entire unsaturated domain. To date, the VMS has been
99	successfully implemented in numerous studies on water flow and contaminant
100	transport in the unsaturated zone in a variety of hydrological setups, including: (i)
101	floodwater percolation in arid environments (Dahan et al., 2007, 2008, 2009), (ii)
102	rainwater percolation through thick sand and clay formations (Rimon et al., 2007;
103	Baram et al., 2012; Turkeltaub et al., 2015a), (iii) solute transport in the vadose zone
104	(Rimon et al., 2011; Baram et al., 2013; Dahan et al., 2014; Turkeltaub et al., 2014,
105	2015b), and (iv) impact of agriculture on groundwater quality (Turkeltaub et al.,
106	2014, 2015b).
107	A VMS was installed under a commercial crop field to study water flow and
108	nitrate transport through the deep vadose zone with respect to rain pattern as well as

1 109 the agricultural and fertilization setup. Continuous data on variations in the sediment 110 water content and nitrate concentrations were collected from the entire vadose zone (18 m deep) for over 6 years. The temporal variations in the vadose zone sediment 111 112 water content were used to evaluate the link between rain pattern and water fluxes (Turkeltaub et al., 2014). The nitrate concentration time series, which included 113

variation of nitrate in time and at multiple depths, revealed, in real time, a major pulse 114





115	of nitrate mass propagating down through the vadose zone toward the water table.
116	Stable nitrate isotope analysis identified the source of the nitrate in the subsurface.
117	The vertical transport properties and total nitrate mass in the vadose zone were
118	estimated according to the transient data. Results from the long-term monitoring were
119	compared with earlier modeling efforts applied at the same site (Turkeltaub et al.,
120	2014).
121	
122	2 Methods
123	
124	2.1 Study area
125	
126	The study was conducted under a commercial crop field located in the
127	southern part of the coastal plain of Israel and situated on the outcrops of a phreatic
128	aquifer (34°41'13" E; 31°49'42" N). Mediterranean climate prevails in this area, with
129	hot, dry summers (May-September) and rainy winters (October-April), an average
130	annual rainfall of 512 mm and average temperatures of 31.2 $^{\circ}\text{C}$ (August) and 17.8 $^{\circ}\text{C}$
131	(January) in the hottest and coldest month, respectively (Israeli Meteorological
132	Service, 2015). Reference evapotranspiration rates calculated according to the
133	Penman-Monteith method (suggested by the Food and Agriculture Organization)
134	range from 1.5 mm/day (January) to 5.7 mm/day (July) (Israeli Meteorological
135	Service, 2015).
136	From 2009 to 2013, the crop field site was cultivated with rainfed winter
137	crops—spring wheat (Triticum aestivum L.) and pea (Pisum sativum L.) (Fig. 1).
138	Then, for 1 year (2013/2014), the field was fallow. The crops were sown at the
139	beginning of the wet season (November) and grew into the spring (April) with no





- 140 additional irrigation. After harvest, plowing practice was implemented. Main
- 141 fertilization application to the crop field was dairy-farm slurry manure. In September
- 142 2014, due to a change in the agricultural cultivation type, jojoba (Simmondsia
- 143 *chinensis*) shrubs were planted, irrigation systems were installed, and the distribution
- 144 of manure ceased.
- 145
- 146 **2.2 Monitoring setup**
- 147

148	The crop field site was selected as representative of the prevalent agricultural
149	setting on the aquifer outcrops and was instrumented with a VMS (Fig. 1). Full
150	technical descriptions of the VMS structure, performance and installation procedures
151	can be found in other publications (Rimon et al., 2007, 2011; Dahan et al., 2008,
152	2009). For brevity, only a general description is given here.
153	The VMS is composed of a flexible sleeve installed in uncased slanted (35°)
154	boreholes hosting multiple monitoring units at various depths. Each monitoring unit
155	has a flexible time-domain reflectometry (FTDR) sensor for continuous measurements
156	of sediment water content, and vadose-zone sampling ports (VSPs) for frequent
157	collection of pore-water samples from the unsaturated zone (Table 1). The slanted
158	installation ensures that each monitoring unit faces an undisturbed sediment column
159	that extends from land surface to the probe or sampling port depth. After insertion of
160	the VMS into the borehole, the flexible sleeve is filled with a high-density solidifying
161	material-liquid two-component urethane-that solidifies in the borehole shortly after
162	its application, thereby ensuring proper sleeve expansion for attachment of the
163	monitoring units to the borehole's irregular walls, sealing its entire void and
164	preventing potential cross-contamination by preferential flow along the borehole.





165	The VMS under the crop field included eight monitoring units distributed
166	vertically and laterally along the entire vadose zone cross section from a depth of 1 m
167	to a depth of 18 m. Note that each monitoring unit is shifted vertically and
168	horizontally from the others along the slanted orientation of the installation (Fig. 1).
169	Since each monitoring unit is located under its own undisturbed sediment column, the
170	integrated data from the VMS should be regarded as representative of a wider zone
171	rather than a single vertical profile. Sediment water content was monitored daily. The
172	pore-water sampling campaigns were conducted every 90 days on average.
173	
174	2.3 Nitrate-transport simulations
175	
176	The observed nitrate concentration dynamics at the 6.3 m depth (Table 1) was
177	analyzed and compared with earlier modeling estimations conducted according to
178	observations of water content under the crop field (Turkeltaub et al., 2014). Nitrate
179	transport was modeled in terms of the convection-dispersion equation (CDE)
180	equilibrium assuming resident concentration for a third-type inlet condition as follows
181	(Toride et al., 1999):
182	$R\frac{\partial c}{\partial t} = D\frac{\partial^2 c}{\partial x^2} - v\frac{\partial c}{\partial x} $ (1)
183	where $c$ is the solution concentration, $x$ is distance, $t$ is time, $D$ is the dispersion
184	coefficient, $v$ is the average pore water velocity (water flux $q$ divided by the water
185	content $\theta$ ), and <i>R</i> is the retardation factor.
186	The nitrate concentrations obtained by the VSP located at the 4.2 m depth (Table 1)
187	served as a series of successive applications of solute pulses (multi-pulse boundary
400	
188	condition). Both VSPs were located in a relatively homogeneous medium of sandy





- 190 model homogeneity. The CXTFIT2 code (Toride et al., 1999) and the Levenberg-
- 191 Marquardt-type optimization approach (Marquardt, 1963), both included in
- 192 STANMOD (van Genuchten et al., 2012), were used for inversely estimating the
- 193 pore-water velocity (v) and dispersion coefficient (D) according to observed
- 194 concentrations. Both parameters were obtained by running CXTFIT2 multiple times
- 195 for inverse optimization, each time with different initial values (Turkeltaub et al.,
- 196 2015a,b).
- 197

#### 198 2.4 Total nitrate mass

199

200 The total nitrate mass in the unsaturated zone estimations was calculated to 201 emphasize the nitrate mass that will eventually contaminate the groundwater. The 202 following equation was used for yearly nitrate mass (per area) in the vadose zone:

$$M = \int_{Z=water_table}^{Z=ground_surface} K_i \times dz_i$$
(2)

where *M* is nitrate mass in the vadose zone under a unit area, *i* indexes the depth interval for which the corresponding VSP is at its centre,  $C_i$  is the nitrate concentration [M/L<sup>3</sup>] sampled with the VSP at that depth interval,  $\theta i$  is the average water content measured by the nearest FTDR sensor, and  $dz_i$  is the interval length (Fig. 2). **3 Results and discussion** 

211

#### 212 **3.1** Nitrate migration in the unsaturated zone





	adose zone of the crop field. The continuous d temporal variations in measured water toring period, most of the rainstorms caused a
216 monitoring of the vadose zone indicated	•
	toring period, most of the rainstorms caused a
217 contents (Fig. 2). Throughout the monit	
rise in the water content measured by th	ne shallowest water sensor (0.5 m, Fig. 2). At
the 2.1 m and 3.1 m depths, the rise in v	water contents corresponded mainly to
significant rain events (Fig. 2b,c). The	sensors at the deeper depths displayed temporal
variability with respect to the cumulativ	ve annual rain pattern. In some years, a lag
between the end of the rainy season and	d the rise in water content was recorded,
223 whereas in other years, the rise in water	r content occurred throughout the entire vadose
224 zone following a significant rain event	(Fig. 2d–h). A more detailed description of the
sequential rise in water content with de	pth following a wetting event on land surface,
and a clear indication of propagation of	a wetting wave down through the vadose zone
227 are presented in our earlier study at the	site (Turkeltaub et al., 2014), and in other
studies at different sites as well (Rimon	a et al., 2007, 2011; Dahan et al., 2008, 2009;
229 Baram et al., 2012, 2013).	
230 During the monitoring period, s	lurry from a nearby dairy farm was often
spread over the field, serving as a nitrog	gen source (Fig. 1). This practice was stopped
in 2014 when the agricultural setting in	the field was changed to a jojoba orchard. The
233 dairy slurry was distributed throughout	May and June, 60 days after harvesting, and
was scattered across the crop field.	
A time series of nitrate concentr	rations at various depths under the field was
236 obtained by frequent sampling of the va	adose zone pore water using the VSPs at
237 multiple depths (Fig. 3). Throughout 6	years of continuous monitoring, different
238 scales and magnitudes of the variations	in nitrate concentration were observed. An





239	overview of the nitrate concentration time series with depth (Fig. 3) reveals a major
240	pulse of elevated concentrations, initiating close to the surface, and gradually
241	progressing down the vadose zone toward the water table at a depth of $\sim 18$ m. The
242	process was first monitored at the uppermost VSP at 1 m depth, where nitrate
243	concentrations displayed a significant increase during the winter of 2010/2011. Then a
244	gradual trend of reduction in nitrate concentration was observed at this depth until
245	March 2014. A close examination of the nitrate concentrations at the 1 m depth
246	indicated repeating fluctuations, high nitrate concentrations after harvest times due to
247	application of the dairy slurry, and then a reduction in concentrations. Although hard
248	to notice at the illustrated scale, the nitrate concentrations between September 2009
249	and September 2010 were still relatively high and fluctuated around $\sim$ 600 mg/L (Fig.
250	3a). Then they escalated to $\sim$ 3200 mg/L after cultivation of the pea crop. Following
251	this tremendous increase in nitrate concentration in May 2011, a decline was observed
252	until January 2012, to ~1500 mg/L (Fig. 3a). This phenomenon repeated itself in April
253	2012, when the nitrate concentration increased again to 2800 mg/L and then decreased
254	to the lower value of 78 mg/L in April 2015 due to cessation of slurry application.
255	Thus, application of dairy farm slurry combined with a legume crop (pea) seemed to
256	have enriched the top soil with excess nitrogen, compared to cultivation of cereal-type
257	crops.
258	Progression of the nitrate migration across deeper parts of the vadose zone
259	could be divided into two periods (Fig. 3). In the first period, October 2010 to January
260	2013, at depths of 2.7 m, 4.2 m, 9.5 m and 15.6 m (Fig. 3b,c,e,g), the escalation in
261	nitrate concentration was moderate and continuous, whereas at depths of 6.3 m and 18
262	m, there was no significant change in nitrate concentrations during this period (Fig.
263	3d,h). In the second period starting from July 2013, following the wet season of





264	2012/13, substantial nitrate breakthroughs were noticeable throughout most of the
265	vadose zone cross section (marked with arrows on Fig. 3). This rapid nitrate
266	progression to the deeper parts of the vadose zone could be related to the soil's
267	physical characteristics. In the top 3 m, the soil domain is comprised of fine-textured
268	layers (sandy-loam and loamy sand), and from 3 m down to 18 m (water table), the
269	soil consists of a coarser sand-textured layer (Turkeltaub et al., 2014). Thus, as a
270	consequence of substantial water percolation, which induced intensive water flux
271	across the coarse-textured soil, nitrate transport could be detected at deeper depths of
272	the vadose zone.
273	
274	3.2 Nitrate sources
275	
276	Nitrate isotope composition in the vadose zone pore water depends on nitrogen
276 277	Nitrate isotope composition in the vadose zone pore water depends on nitrogen sources and transformation processes (Böhlk, 2002). Moreover, it can provide an
277	sources and transformation processes (Böhlk, 2002). Moreover, it can provide an
277 278	sources and transformation processes (Böhlk, 2002). Moreover, it can provide an indication of downward transport rates within the vadose zone (Turkeltaub et al.,
277 278 279	sources and transformation processes (Böhlk, 2002). Moreover, it can provide an indication of downward transport rates within the vadose zone (Turkeltaub et al., 2015b). Nitrogen isotopic signature analyses were conducted on water samples
277 278 279 280	sources and transformation processes (Böhlk, 2002). Moreover, it can provide an indication of downward transport rates within the vadose zone (Turkeltaub et al., 2015b). Nitrogen isotopic signature analyses were conducted on water samples extracted by the VSPs (Fig. 4). The $\delta^{15}$ N values clearly showed that manure is the
277 278 279 280 281	sources and transformation processes (Böhlk, 2002). Moreover, it can provide an indication of downward transport rates within the vadose zone (Turkeltaub et al., 2015b). Nitrogen isotopic signature analyses were conducted on water samples extracted by the VSPs (Fig. 4). The $\delta^{15}$ N values clearly showed that manure is the main source of nitrate in the vadose zone pore water (Fig. 4). Moreover, these values
277 278 279 280 281 282	sources and transformation processes (Böhlk, 2002). Moreover, it can provide an indication of downward transport rates within the vadose zone (Turkeltaub et al., 2015b). Nitrogen isotopic signature analyses were conducted on water samples extracted by the VSPs (Fig. 4). The $\delta^{15}$ N values clearly showed that manure is the main source of nitrate in the vadose zone pore water (Fig. 4). Moreover, these values suggested that transformation processes such as nitrification and mineralization of soil
277 278 279 280 281 282 283	sources and transformation processes (Böhlk, 2002). Moreover, it can provide an indication of downward transport rates within the vadose zone (Turkeltaub et al., 2015b). Nitrogen isotopic signature analyses were conducted on water samples extracted by the VSPs (Fig. 4). The $\delta^{15}$ N values clearly showed that manure is the main source of nitrate in the vadose zone pore water (Fig. 4). Moreover, these values suggested that transformation processes such as nitrification and mineralization of soil nitrogen sources have little effect on nitrate isotopic signature. Nitrate seems to
277 278 279 280 281 282 283 283	sources and transformation processes (Böhlk, 2002). Moreover, it can provide an indication of downward transport rates within the vadose zone (Turkeltaub et al., 2015b). Nitrogen isotopic signature analyses were conducted on water samples extracted by the VSPs (Fig. 4). The $\delta^{15}$ N values clearly showed that manure is the main source of nitrate in the vadose zone pore water (Fig. 4). Moreover, these values suggested that transformation processes such as nitrification and mineralization of soil nitrogen sources have little effect on nitrate isotopic signature. Nitrate seems to behave like a conservative ion in most parts of the vadose zone and there is relatively





- 288 deep vadose zone demonstrated a leaching process and migration of a nitrate plume
- from the soil surface toward the groundwater.

290

- 291 **3.3** Nitrate storage in the vadose zone
- 292

293 Total nitrate mass in the unsaturated zone (as calculated by equation 2) 294 indicates the nitrate's fate in the vadose zone under the crop field (Fig. 5). The mass calculation is based on the concentration time series from eight points across the 295 296 unsaturated zone. Initially, the yearly nitrate mass calculations displayed a drastic 297 increase in 2010, at the same time as its identification in the upper part of the vadose zone (Fig. 3a). Subsequently, the highest increase in nitrate mass was calculated for 298 2011 following the combination of cultivation of a legume crop type and excessive 299 application of dairy slurry (Fig. 5). It seems that the yearly fluctuations in calculated 300 nitrate mass can be explained by the lag time in the transport process between the 301 302 sampling points. Hence, the peak in nitrate mass observed in the upper parts during 303 2011 (Fig. 5) remained in the vadose cross section and reached the deeper parts of the 304 vadose zone as a breakthrough. 305 306 3.4 Validity of the transport model

307

To verify that the observed dynamics of the nitrate concentrations compare with earlier numerical model simulation results (Turkeltaub et al., 2014), the porewater velocity and the hydrodynamic dispersion were inversely estimated by solving the analytical solution for the CDE (equation 1) (Fig. 6). The observed nitrate concentrations at the 4.2 m depth (Fig. 3c) were used as the nitrate source and input to





313	the model in multi-pulse manner, and the CDE was calibrated according to nitrate
314	concentrations obtained at the 6.3 m depth (Fig. 3d). Close examination of the results
315	indicated relatively good agreement between observed and simulated nitrate
316	concentration trends (Fig. 6). Nevertheless there were discrepancies in the absolute
317	values, with the simulated nitrate concentrations increasing before the observed
318	concentrations. These gaps could be explained by the assumptions that are intrinsic to
319	the CDE model-homogeneous medium and average velocity-along with the
320	assumption of even distribution of the nitrogen source on the surface. However, none
321	of these assumptions could be found in the field. Nevertheless, the CDE provided an
322	approximation that could be compared with earlier numerical modeling results. The
323	calculated hydrodynamic dispersion was 50 $\mathrm{cm}^2/\mathrm{day}$ and the pore-water velocity was
324	0.915 cm/day, which is ~333.97 cm/year. Multiplying the velocity by the average
325	water content observed at 3.1 m, ~0.075 $\text{cm}^3/\text{cm}^3$ (Fig. 2c), the Darcian flux equaled
326	~25 $\pm$ 9 cm/year, which is an underestimation of the earlier average flux estimation of
327	19.9 cm/year averaged over 24 years (Turkeltaub et al., 2014).
328	
329	3.5 Practical implications of vadose-zone monitoring
330	
331	There is much evidence indicating that agricultural practices have led to
332	alterations in unsaturated sediment pore-water chemicals. Moreover, agricultural land
333	use is one of the major non-point sources for groundwater contamination, in particular
334	contamination by nitrate. To prevent a long-term gradual degradation in groundwater
335	quality, the link between sources of pollution on the surface and their migration
336	pattern in the unsaturated zone should be understood long before their final
227	

337 cumulative imprint in the aquifer water. Today's wide use of nitrate detection in





338	groundwater by standard traditional monitoring wells might be misleading due to the
339	mixing of waters from uncultivated and cultivated areas, which results in lower nitrate
340	concentrations and masks the pollution process. Hence, protection of groundwater
341	from potential pollution originating from agricultural land uses has to include
342	effective and continuous monitoring of the vadose zone. In this way, pollution events
343	can be monitored in their early stages, long before large-scale nitrate contamination of
344	the groundwater becomes inevitable.
345	Lastly, the VMS presented here was installed under a crop field which was
346	fertilized by the distribution of dairy slurry, a method that is commonly used
347	worldwide. This method, and its potential impact on groundwater contamination, have
348	been previously investigated (e.g. Basnet et al., 2001; Olson et al., 2009; Salazar et
349	al., 2012). However, the results presented here from continuous monitoring of the
350	vadose zone's hydraulic and chemical properties leave no doubt that this method
351	causes groundwater pollution.
352	
353	4 Conclusions
354	• Application of a VMS under an agricultural field enabled real-time tracking of
355	water flow and nitrate transport from the surface through the entire deep
356	vadose zone to the water table at 18 m depth.
357	• The leaching process and migration of a nitrate plume were demonstrated by
358	nitrate concentration time series and water-content measurements from
359	multiple depths in the deep vadose zone underlying a crop field fertilized by
360	dairy slurry application.
361	• Isotopic composition of nitrate in the water samples indicated that manure is
362	the main nitrogen source for nitrate in the vadose-zone pore water. Nitrogen





363	transformation processes such as nitrification and mineralization seem to have
364	only little effect under an intensively fertilized crop field.
365	• Total nitrate mass estimations and simulated pore-water velocity using the
366	analytical solution of the convection-dispersion equation indicated dominance
367	of vertical nitrate transport.
368	• Protection of groundwater from potential pollution originating from
369	agricultural land uses has to include effective and continuous monitoring of
370	the vadose zone. Pollution events can be monitored in their early stages, long
371	before pollution accumulates in the aquifer water.
372	
373	
374	
375	
373	
376	Acknowledgements
	Acknowledgements
376	Acknowledgements This work was funded by the Israel Water Authority (#4500687174). Thanks
376 377	
376 377 378	This work was funded by the Israel Water Authority (#4500687174). Thanks
376 377 378 379	This work was funded by the Israel Water Authority (#4500687174). Thanks go to Sara Elchanani and the Division of Water Quality of the Israel Water Authority
376 377 378 379 380	This work was funded by the Israel Water Authority (#4500687174). Thanks go to Sara Elchanani and the Division of Water Quality of the Israel Water Authority for supporting and funding the project. We wish to express our gratitude to the
376 377 378 379 380 381	This work was funded by the Israel Water Authority (#4500687174). Thanks go to Sara Elchanani and the Division of Water Quality of the Israel Water Authority for supporting and funding the project. We wish to express our gratitude to the farmers who allowed us to conduct this study in their fields. In addition, we would
376 377 378 379 380 381 382	This work was funded by the Israel Water Authority (#4500687174). Thanks go to Sara Elchanani and the Division of Water Quality of the Israel Water Authority for supporting and funding the project. We wish to express our gratitude to the farmers who allowed us to conduct this study in their fields. In addition, we would like to express our appreciation to Michael Kogel for his extensive effort in
376 377 378 379 380 381 382 383	This work was funded by the Israel Water Authority (#4500687174). Thanks go to Sara Elchanani and the Division of Water Quality of the Israel Water Authority for supporting and funding the project. We wish to express our gratitude to the farmers who allowed us to conduct this study in their fields. In addition, we would like to express our appreciation to Michael Kogel for his extensive effort in maintaining and operating the VMS. Data can be obtained by contacting the
376 377 378 379 380 381 382 383 384	This work was funded by the Israel Water Authority (#4500687174). Thanks go to Sara Elchanani and the Division of Water Quality of the Israel Water Authority for supporting and funding the project. We wish to express our gratitude to the farmers who allowed us to conduct this study in their fields. In addition, we would like to express our appreciation to Michael Kogel for his extensive effort in maintaining and operating the VMS. Data can be obtained by contacting the





### 388 References

- 389
- 390 Baram, S., Kurtzman, D., and Dahan, O.: Water percolation through a clayey vadose
- 391 zone, J. Hydrol., 424–425, 165–171, doi:10.1016/j.jhydrol.2011.12.040, 2012.
- 392 Baram, S., Ronen, Z., Kurtzman, D., Kulls, C., and Dahan, O.: Desiccation-crack-
- induced salinization in deep clay sediment, Hydrol. Earth Syst. Sci., 17, 1533–
- 394 1545, doi:10.5194/hess-17-1533-2013, 2013.
- 395 Baram, S., Kurtzman, D., Ronen, Z., Peeters, A., and Dahan, O.: Assessing the impact
- of dairy waste lagoons on groundwater quality using a spatial analysis of vadose
- 397 zone and groundwater information in a coastal phreatic aquifer, J. Environ.
- 398 Manage., 132, 135–144, doi:10.1016/j.jenvman.2013.11.008, 2014.
- 399 Basnet, B. B., Apan, A. A., and Raine, R. R.: Selecting suitable sites for animal waste
- 400 application using a raster GIS, Environ. Manage., 28, 519–531,
- 401 doi:10.1007/s002670010241, 2001.
- 402 Beggs, R. A., Hills, D. J., Tchobanoglous, G., and Hopmans, J. W.: Fate of nitrogen
- 403 for subsurface drip dispersal of effluent from small wastewater systems, J.
- 404 Contam. Hydrol., 126(1–2), 19–28, doi:10.1016/j.jconhyd.2011.05.007, 2011.
- 405 Böhlke, J. K.: Groundwater recharge and agricultural contamination, Hydrogeol.
- 406 J., 10, 153–179, 2002.
- 407 Botros, F. E., Onsoy, Y. S., Ginn, T. R., and Harter, T.: Richards equation-based
- 408 modeling to estimate flow and nitrate transport in a deep alluvial vadose zone,
- 409 Vadose Zone J., 11(4), doi:10.2136/vzj2011.0145, 2012.
- 410 Dahan, O., Shani, Y., Enzel, Y., Yechieli, Y., and Yakirevich, A.: Direct
- 411 measurements of floodwater infiltration into shallow alluvial aquifers, J.
- 412 Hydrol., 344, 157–170, doi:10.1016/j.jhydrol.2007.06.033, 2007.





413	Dahan, O., Tatarsky, B., Enzel, Y., Kulls, C., Seely, M., and Benito, G.: Dynamics of	
414	flood water infiltration and ground water recharge in hyperarid desert, Ground	
415	Water, 46, 450-461, doi:10.1111/j.1745-6584.2007.00414, 2008.	
416	Dahan, O., Talby, R., Yechieli, Y., Adar, E., Lazarovitch, N., and Enzel, Y.: In situ	
417	monitoring of water percolation and solute transport using a vadose zone	
418	monitoring system, Vadose Zone J., 8, 916-925, doi:10.2136/vzj2008.0134,	
419	2009.	
420	Dahan, O., Babad, A., Lazarovitch, N., Russak, E. E., and Kurtzman, D.: Nitrate	
421	leaching from intensive organic farms to groundwater, Hydrol. Earth Syst. Sci.,	
422	18, 333-341, doi:10.5194/hess-18-333-2014, 2014.	
423	Dann, R., Bidwell, V., Thomas, S., Wöhling, T., and Close, M.: Modeling of	
424	nonequilibrium bromide transport through alluvial gravel vadose zones, Vadose	
425	Zone J., 9, 731–746, doi:10.2136/vzj2009.0127, 2010.	
426	Dejwakh, N. R., Meixner, T., Michalski, G., and Mcintosh, J.: Using <sup>17</sup> O to	
427	investigate nitrate sources and sinks in a semi-arid groundwater system,	
428	Environ. Sci. Technol., 46, 745–751, dx.doi.org/10.1021/es203450z, 2012.	
429	Doltra, J., and Muñoz, P.: Simulation of nitrogen leaching from a fertigated crop	
430	rotation in a Mediterranean climate using the EU-Rotate_N and Hydrus-2D	
431	models, Agric. Water Manage., 97, 277-285, doi:10.1016/j.agwat.2009.09.019,	
432	2010.	
433	European Community: Council directive concerning the protection of water against	
434	pollution caused by nitrates from agricultural sources, Official Journal of the	
435	European Community (91/676/EEC), Legislation 1375/1-375/8, European	
436	Community, 1991.	





- 437 Elhanany, S.: Challenges in preserving the quality of water resources in Israel, The
- 438 Jerusalem Conference for Environment and Nature, Jerusalem (in Hebrew),
- 439 2009.
- 440 Green, C. T., Fisher, L. H., and Bekins, B. A.: Nitrogen fluxes through unsaturated
- 441 zones in five agricultural settings across the United States, J. Environ. Qual., 37,
- 442 1073–1085, doi:10.2134/jeq2007.0010, 2008.
- 443 Hanson, B. R., Šimůnek, J., and Hopmans, J. W.: Evaluation of urea-ammonium-
- 444 nitrate fertigation with drip irrigation using numerical modeling, Agric. Water

445 Manage., 86, 102–113, doi:10.1016/j.agwat.2006.06.013, 2006.

- 446 Israel Meteorological Service: Web Israel Meteorological Service: data base.
- 447 <a href="http://data.gov.il/ims-results">http://data.gov.il/ims-results</a> (accessed 1 Dec 2015).
- 448 Kaplan, N., and Magaritz, M.: A nitrogen-isotope study of the sources of nitrate
- 449 contamination in groundwater of the Pleistocene coastal plain aquifer, Israel,
- 450 Water Res., 20, 131–135, 1986.
- 451 Kurtzman, D., Shapira, R. H., Bar-Tal, A., Fine, P., and Russo, D.: Nitrate fluxes to
- 452 groundwater under citrus orchards in a Mediterranean climate: observations,
- 453 calibrated models, simulations and agro-hydrological conclusions, J. Contam.

454 Hydrol., 151(3), 93–104, doi:10.1016/j.jconhyd.2013.05.004, 2013.

455 Leenhardt, D., Lafolie, F., and Bruckler, L.: Evaluating irrigation strategies for lettuce

- 456 by simulation: 1. Water flow simulations, Eur. J. Agron., 8, 249–265, 1998a.
- 457 Leenhardt, D., Lafolie, F., Bruckler, L., and de Cockborne A.-M.: Evaluating
- 458 irrigation strategies for lettuce by simulation: 2. Nitrogen budget, Eur. J. Agron.,
- 459 8, 267–282, 1998b.
- 460 Marquardt, D. W.: An algorithm for least-squares estimation of nonlinear parameters,
- 461 SIAM J. Appl. Math., 11, 431–441, 1963.





462	Nolan, B. T., Puckett, L. J., Ma, L., Green, C. T., Bayless, E. R., and Malone, R. W.:
463	Predicting unsaturated zone nitrogen mass balances in agricultural settings of
464	the United States, J. Environ. Qual., 39, 1051–1065, doi:10.2134/jeq2009.0310,
465	2010.
466	Olson, B. M., Bennett, D. R., McKenzie, R. H., Ormann, T. D., and Atkins, R. P.:
467	Nitrate leaching in two irrigated soils with different rates of cattle manure, J.
468	Environ. Qual., 38, 2218-2228, doi:10.2134/jeq2008.0519, 2009.
469	Onsoy, Y. S., Harter, T., Ginn, T. R., and Horwath, W. R.: Spatial variability and
470	transport of nitrate in a deep alluvial vadose zone, Vadose Zone J., 4, 41-54,
471	2005.
472	Oren, O., Yechieli, Y., Böhlke, J. K., and Dody, A.: Contamination of groundwater
473	under cultivated fields in an arid environment, central Arava Valley, Israel, J.
474	Hydrol., 290, 312–328, doi:10.1016/j.jhydrol.2003.12.016, 2004.
475	Rimon, Y., Dahan, O., Nativ, R., and Geyer, S.: Water percolation through the deep
476	vadose zone and groundwater recharge: Preliminary results based on a new
477	vadose zone monitoring system, Water Resour. Res., 43, W05402,
478	doi:10.1029/2006WR004855, 2007.
479	Rimon, Y., Nativ, R., and Dahan, O.: Physical and chemical evidence for pore-scale
480	dual-domain flow in the vadose zone, Vadose Zone J., 9, 1-10,
481	doi:10.2136/vzj2009.0113, 2011.
482	Rupert, M. G.: Decadal-scale changes of nitrate in ground water of the United States,
483	1988–2004, J. Environ. Qual., 37, 240–248, doi:10.2134/jeq2007.0055, 2008.
484	Salazar, F., Martínez-Lagos, J., Alfaro, M., and Misselbrook, T.: Low nitrogen
485	leaching losses following a high rate of dairy slurry and urea application to





- 486 pasture on a volcanic soil in Southern Chile, Agr. Ecosys. Environ., 160, 23–28,
- 487 doi:10.1016/j.agee.2012.04.018, 2012.
- 488 Scanlon, B. R., Reedy, R. C., Gates, J. B., and Gowda, P. H.: Impact of
- 489 agroecosystems on groundwater resources in the Central High Plains, USA, Agr
- 490 .Ecosys. Environ., 139, 700–713, 2010.
- 491 Showers, W. J., Genna, B., McDade, T., Bolich, R., and Fountain, J. C.: Nitrate
- 492 contamination in groundwater on an urbanized dairy farm, Environ. Sci.
- 493 Technol., 42, 4683–4688, 2008.
- 494 Spalding, R. F., Watts, D. G., Schepers, J. S., Burbach, M. E., Exner, M. E., Poreda,
- 495 R. J., and Martin, G. E.: Controlling nitrate leaching in irrigated agriculture, J.
- 496 Environ. Qual., 30, 1184–1194, 2001.
- 497 Toride, N., Leij, F. J., and van Genuchten, M. Th.: The CXTFIT code for estimating
- transport parameters from laboratory or field tracer experiments, Version 2.1,
- 499 Research Report No. 137, USDA-ARS US Salinity Laboratory, Riverside, CA,
- 500 USA, 1999.
- 501 Turkeltaub, T., Dahan, O., and Kurtzman, D.: Investigation of groundwater recharge
- 502 under agricultural fields using transient deep vadose zone data, Vadose Zone J.,
- 503 13, 1–13, doi:10.2136/vzj2013.10.0176, 2014.
- 504 Turkeltaub, T., Kurtzman, D., Bel, G., and Dahan, O.: Examination of groundwater
- 505 recharge with a calibrated/validated flow model of the deep vadose zone, J.
- 506 Hydrol., 522, 618–627, doi:10.1016/j.jhydrol.2015.01.026, 2015a.
- 507 Turkeltaub, T., Kurtzman, D., Russak, E. E., and Dahan, O.: Impact of switching crop
- 508 type on water and solute fluxes in deep vadose zone, Water Resour. Res., 51,
- 509 9828–9842, doi:10.1002/2015WR017612, 2015b.





510	US EPA, Is your drinking water safe? EPA, Office of Water (publication number 810
511	F94002, 1994), 2015. Available from http://www.epa.gov/nscep/index. html
512	(October 2015).
513	Van Genuchten, M. Th., Šimůnek, J., Leij, F. J., Toride, N., and Šejna, M.:
514	STANMOD: model use, calibration and validation, Trans, ASABE 55, 1353-
515	1366, 2012.
516	Wassenaar, L. I.: Evaluation of the origin and fate of nitrate in the Abbotsford Aquifer
517	using the isotopes of <sup>15</sup> N and <sup>18</sup> O in NO <sub>3</sub> , Appl. Geochem., 10, 391–405,
518	doi:10.1016/0883-2927(95)00013-A, 1995.
519	Wassenaar, L. I., Hendry, M. J., and Harrington, N.: Decadal geochemical and
520	isotopic trends for nitrate in a transboundary aquifer and implications for
521	agricultural beneficial management practices, Environ. Sci. Technol., 40, 4626-
522	4632, 2006.
523	
524	
525	
526	
527	
528	
529	
530	
531	
532	
533	
534	





542

535	
536	
537	
538	Table 1
539	Depth distribution of the vadose-zone monitoring system (VMS) units.

VSP <sup>1,2</sup>	FTDR <sup>1,3</sup>
1	0.5
2.7	2.1
4	3.1
6.3	5.7
9.5	8.9
12.6	12
15.7	15.1
18	17.4

<sup>1</sup> Depth measured relative to land surface at the site.
<sup>2</sup> Vadose zone pore-water sampling port.

<sup>3</sup> Flexible time-domain reflectometry probe.

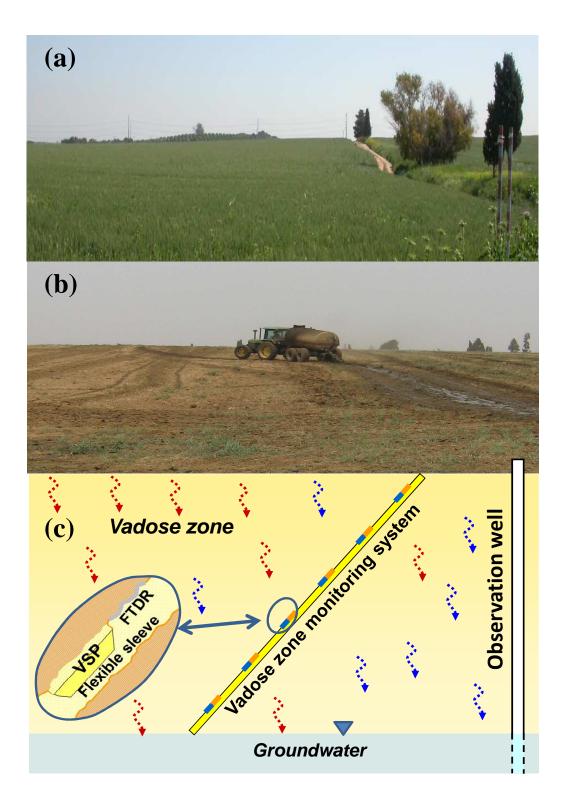




543	Figures
544	
545	Figure. 1. Crop field site with monitoring location during two periods: crop growth
546	during the wet season (a), and after harvesting and during slurry application (b). (c)
547	Schematic illustration of the vadose-zone monitoring system installed under the crop
548	field. VSP, vadose-zone sampling port; FTDR, flexible time-domain reflectometry
549	sensor.
550	
551	<b>Figure. 2.</b> Daily rainfall and water-content $(\theta)$ variations at different depths across the
552	vadose zone as monitored by the flexible time-domain reflectometry sensors.
553	
554	Figure. 3. Daily rainfall and time series of observed nitrate (NO <sub>3</sub> ) concentrations
555	which were obtained by the vadose-zone sampling ports (VSPs) at multiple depths for
556	6 consecutive years.
557	
558	Figure. 4. $\delta^{15}$ N profile of nitrate in the water samples obtained from the vadose zone
559	under the crop field.
560	
561	Figure. 5. Yearly total nitrate mass of the entire vadose zone over the years of
562	sampling.
563	
564	Figure. 6. Observed (red circles) and simulated (dashed blue line) nitrate
565	concentrations for the vadose-zone sampling port (VSP) at the 6.3 m depth. The
566	nitrate concentrations obtained by the VSP at the 4.2 m depth served as a multi-pulse
567	input boundary condition.

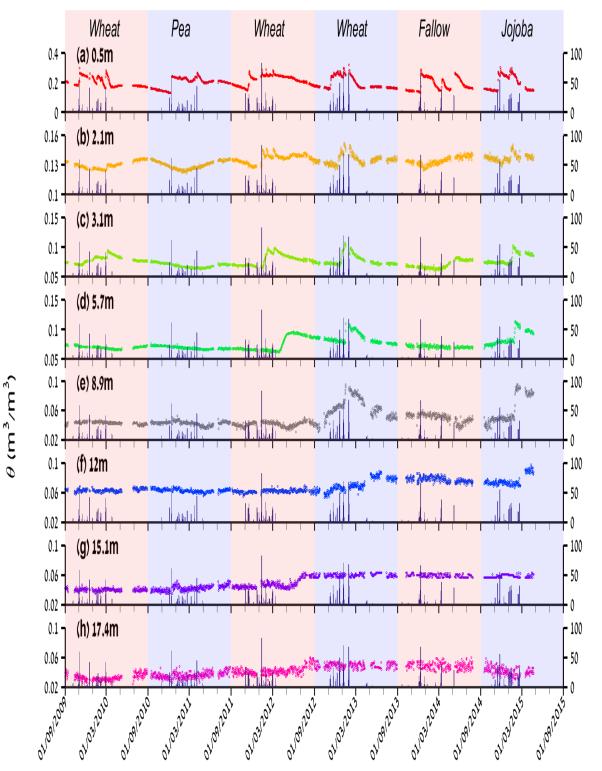








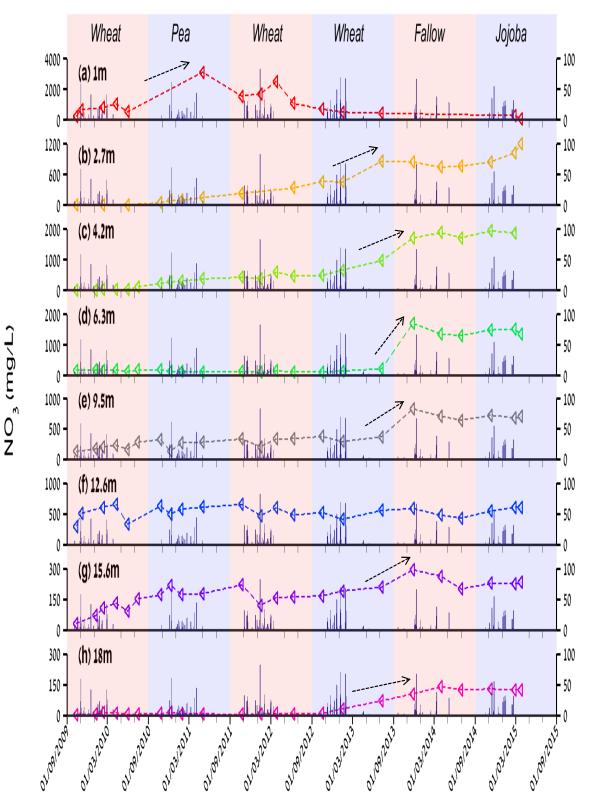




Rain (mm/day)







Rain (mm/day)





